

Seasonality of eddy iron fluxes in the Southern Ocean and its impact on primary production

Takaya Uchida¹, Ryan Abernathy¹, Galen McKinley¹, Shafer Smith², Dhruv Balwada² and Marina Lévy³

1: Lamont-Doherty Earth Observatory, Columbia University, 2: Center for Atmosphere Ocean Science, New York University, 3: Laboratoire d'Océanographie et du Climat

Objectives

We examine the seasonal dynamics in a eddy permitting simulation configured for the Southern Ocean. Seasonally resolved zonal wavenumber power spectra are calculated for eddy kinetic energy (EKE). The EKE spectra consistently show higher power at small scales during winter throughout the domain. Our study looks into:

- Seasonality of EKE and its mechanism.
- Eddy iron fluxes and its impact on primary production.

Introduction

In this study, we investigate seasonal variability in eddy kinetic energy (EKE) in an idealized model configured for the Southern Ocean and couple it to the two-species version of the Darwin biogeochemical model. Seasonality of the dynamics are consistent with available observations and we show how resolving eddy iron fluxes impact the spring bloom of primary production. According to the criteria of *Hallberg et al.* (2013), the 20 km, 5 km (and 1 km currently spinning up)-resolution of our simulation is in the range of mesoscale permitting to resolving. Although this is rather coarse for a regional model, it allows for a direct comparison with global climate models that have roughly 0.1° resolution. Additionally, because of its resolution and dynamical limitations, the analysis of such simulations serves as an experiment into the mechanisms which can drive seasonality.

Model description

The code solves the hydrostatic Boussinesq equations in Cartesian coordinates on the β plane using the Massachusetts Institute of Technology general circulation model (MITgcm). The model domain and surface boundary conditions are shown in Figs. 1 and 2. Since the model domain is a channel, it is configured to represent the *zero-residual* overturning circulation regime.

- $L_x = 1000$ km, $L_y = 2000$ km, $H = 3000$ m.
- Subgrid scale horizontal mixing is parameterized using the Leith scheme.
- The vertical diffusion depends on the K-profile parameterization (KPP).
- The 20 km run has 40 vertical layers (mesoscale permitting) and 5 km run 76 layers (mesoscale resolving).
- No salinity stepping.
- The first deformation wavelength $\lambda_d (= 2\pi R_d)$ is around 100 km.
- Monthly SST relaxation and wind stress forcing are prescribed.

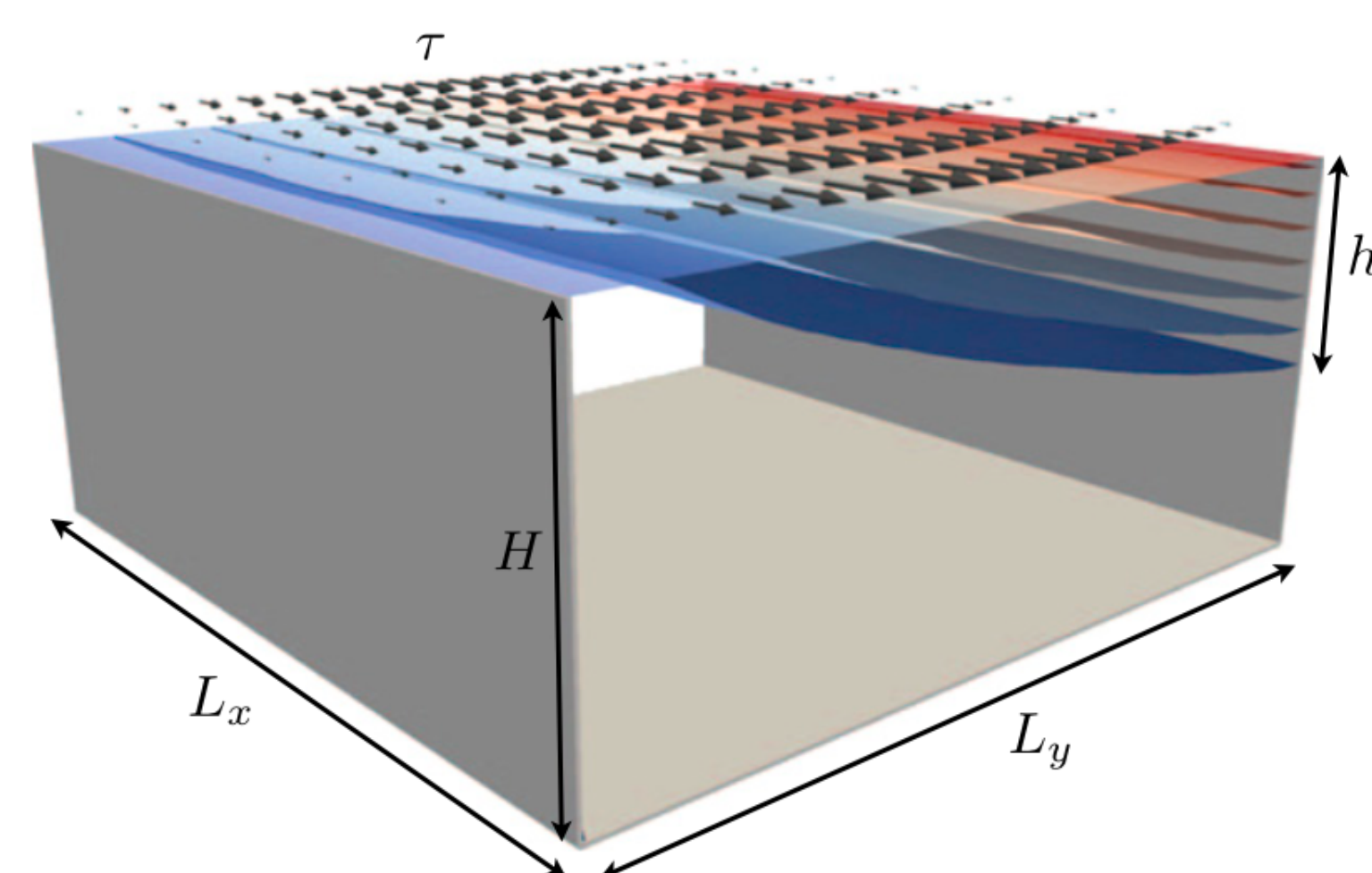


Figure 1: The channel model domain with the size of $L_x = 1000$ km \times $L_y = 2000$ km \times $H = 2985$ m.

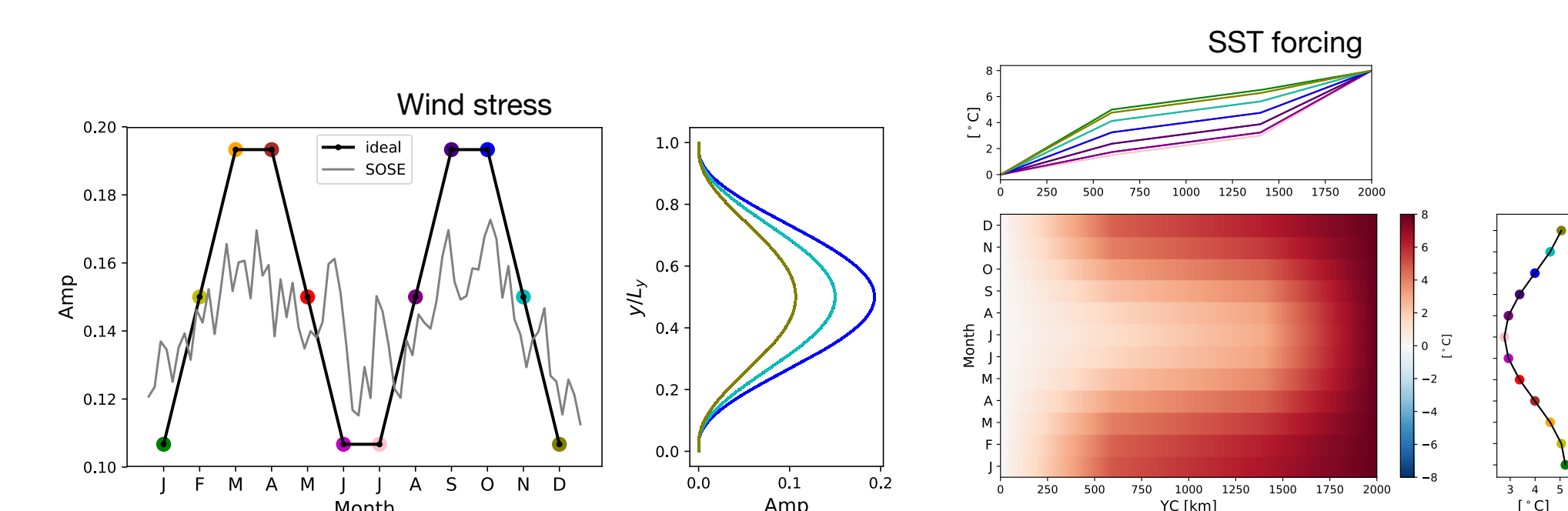


Figure 2: Monthly SST and wind stress forcing.

Climatological outputs

Figure 3 and 4 shows the zonally averaged climatological residual overturning stream function (ψ_{res}) in Sv, and mixing layer depth. The residual overturning is weak due to there being no connection to the northern basins.

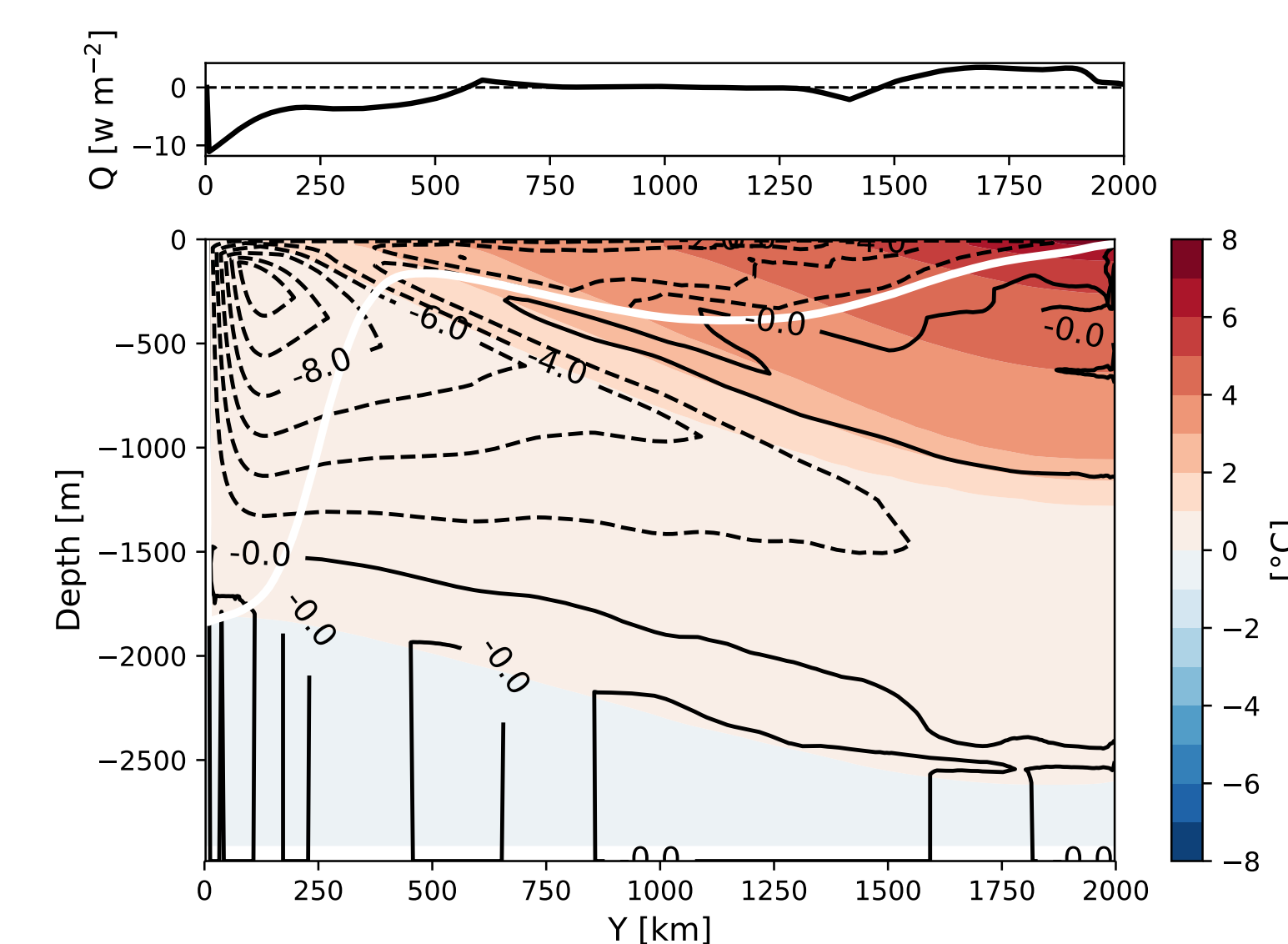


Figure 3: The top panel shows the surface heat flux (Q). The bottom panel shows the buoyancy frequency (N^2 ; in color), residual overturning stream function (ψ_{res} ; black) and the MLD (white).

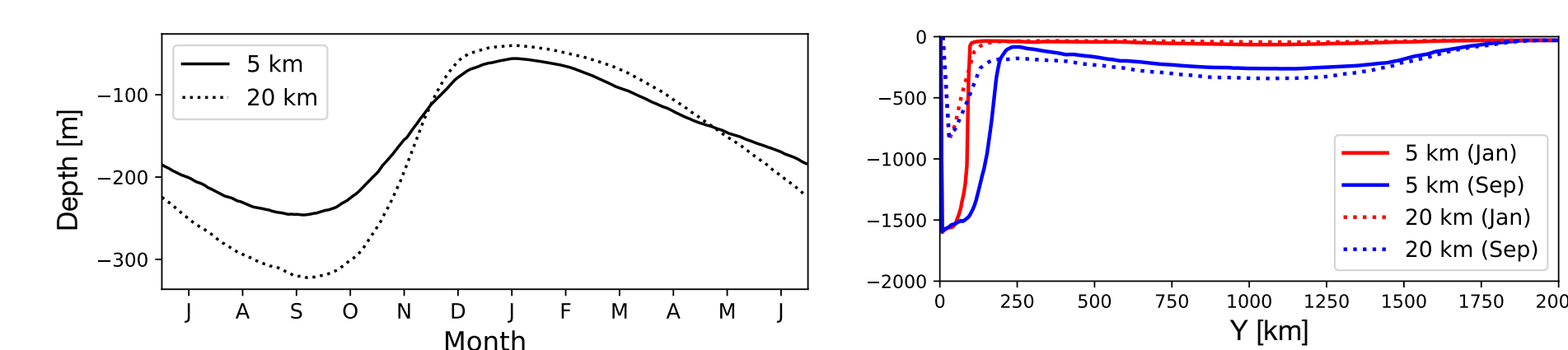


Figure 4: The monthly climatological zonal-mean of MXLD our channel runs plotted against month (left) and meridional distance (right).

Important Result

Seasonality in EKE at scales smaller than 25 km is consistent with the baroclinic energy conversion rates ($\overline{w'b'}$). The spring bloom takes its apex after the MXLD starts to shallow but eddy iron fluxes augment the iron supply over the summer.

Baroclinic instability

The seasonality of $\overline{w'b'}$ is shown in Fig. 6. It is consistent with the seasonality in the CESM runs and interesting to note that the seasonality of energy conversion is largest within the mixing layer.

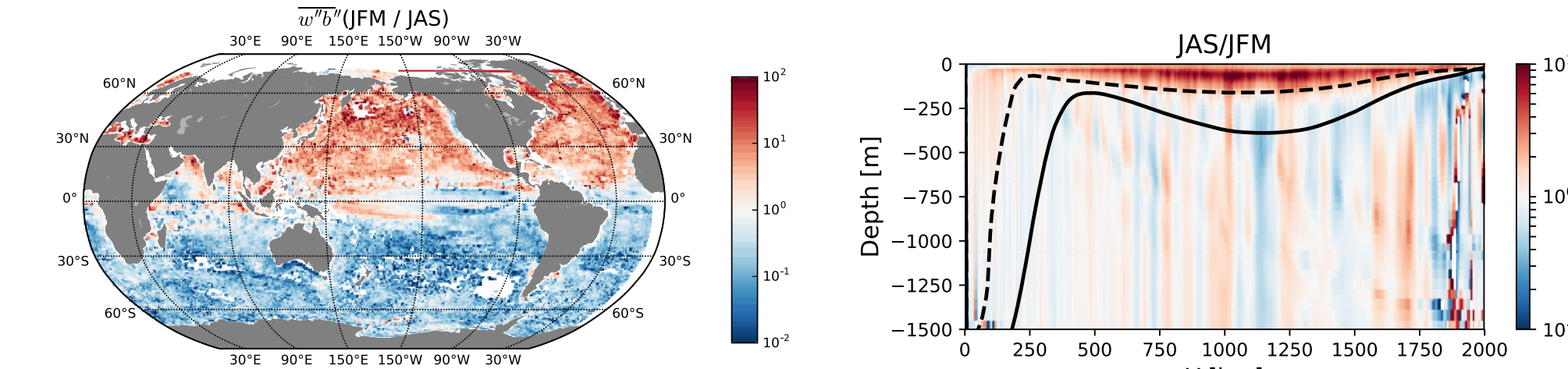


Figure 6: Seasonality of baroclinic energy conversion rate from the 0.1° CESM run and 5 km run.

We show the seasonality of baroclinic instability growth rates of the model in Fig. 7 with the background profiles of zonal-mean seasonal climatological buoyancy frequency and geostrophic velocities at $Y=1250$ km. The large growth rates near the Nyquist wavelength during winter are due to the reduced stratification in the surface layer.

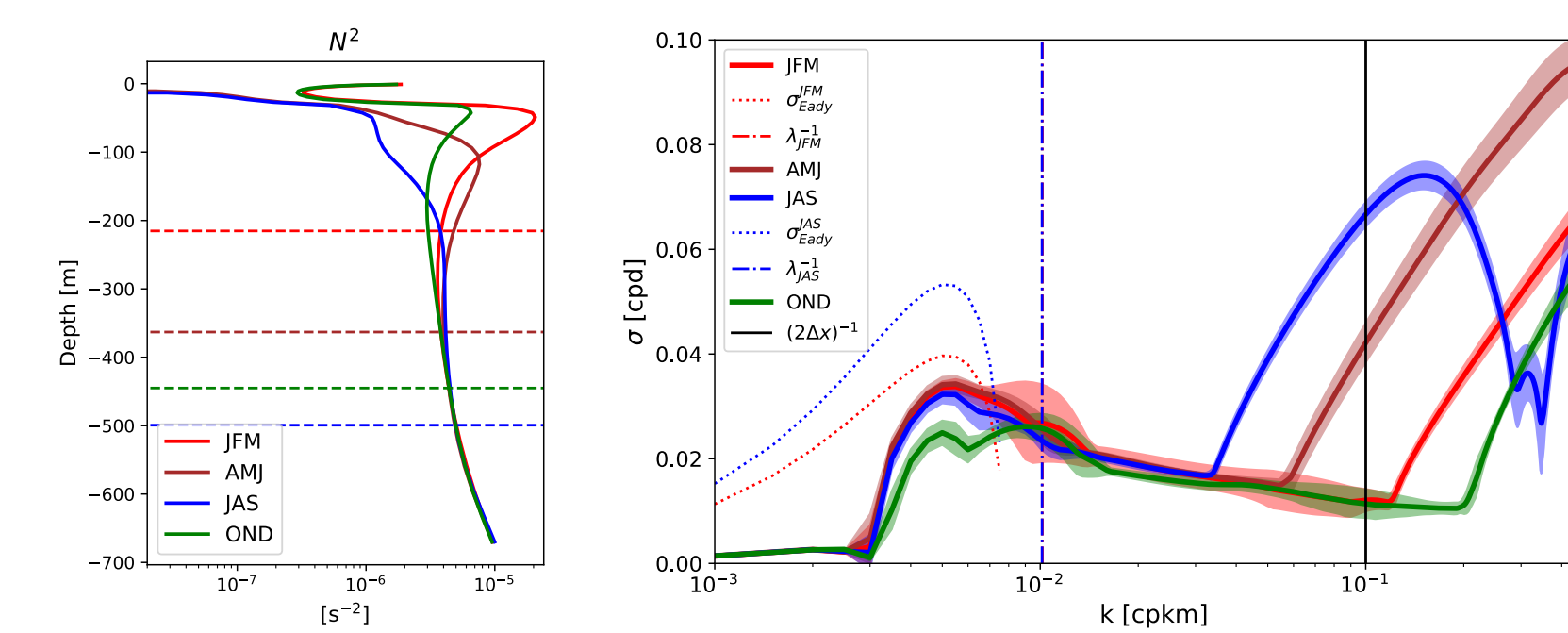


Figure 7: The seasonal Nyquist Frequency and MLD are shown on the left. Baroclinic instability growth rates are plotted against inverse wavelength and the full-depth Eady growth rates are shown in dashed lines respectively.

Seasonality in EKE

Figure 5 shows the zonal wavenumber spectra of surface EKE ($\overline{u'^2 + v'^2}/2$ where the primes denote the deviation from the *seasonal climatology* and zonal mean and the overline denotes a temporal and meridional mean) along with the monthly climatology of EKE, baroclinic energy conversion rates ($\overline{w'b'}$) averaged over the top 100 m, zonal wind stress (τ) and surface heat flux (Q). EKE is higher during winter time compared to summertime at spatial scales of 25 km and smaller (Fig. 5). EKE in the surface layer is in phase with the energy conversion rate within a lag of a month.

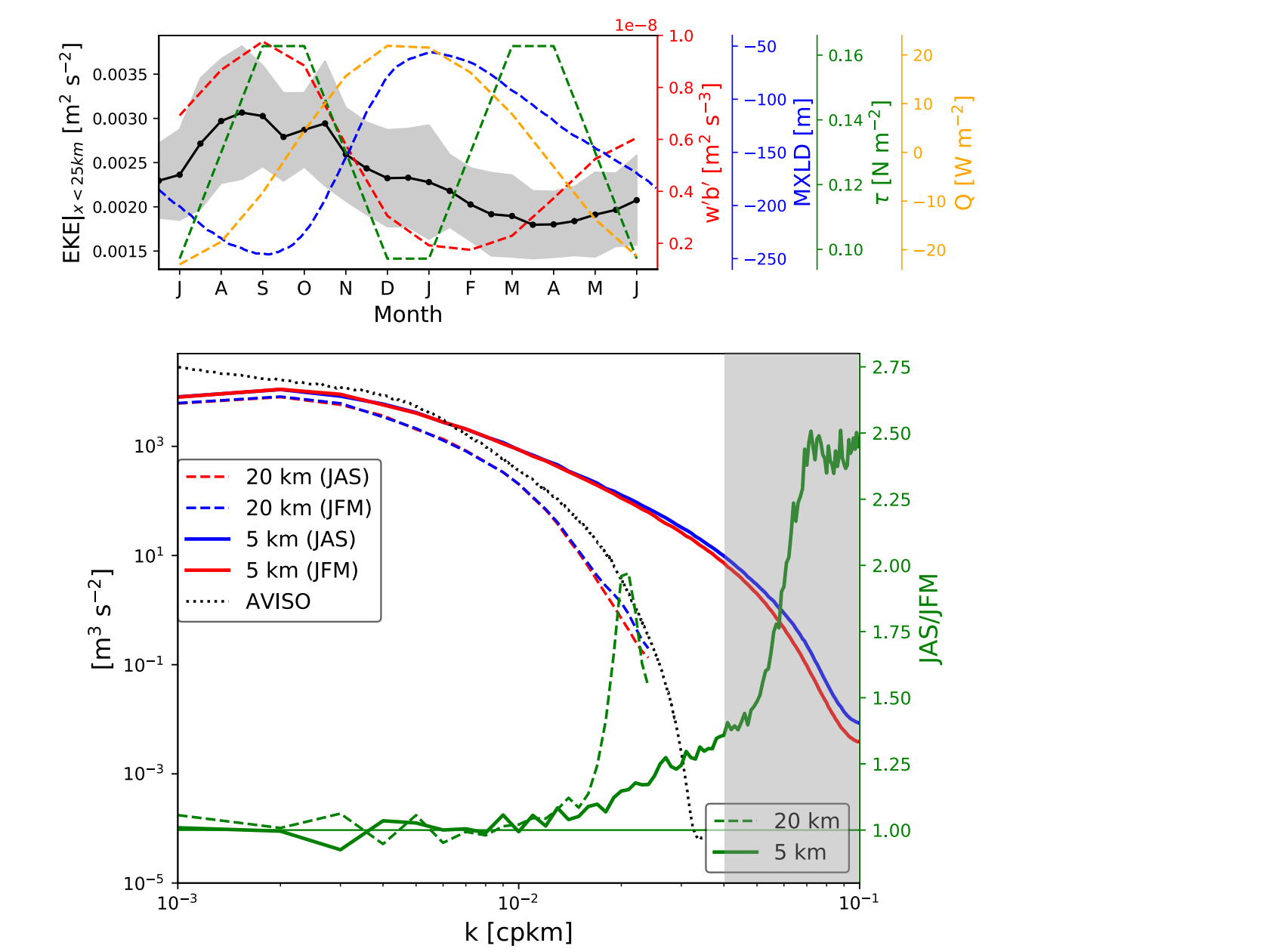


Figure 5: The monthly EKE below scales of 25 km (solid black) and $w'b'$ (dashed black) averaged between $Y=600-1400$ km and $Z=0-100$ m are shown (top panel). Seasonal wavenumber spectra for the channel MOC, AVISO and Jason 2 (right).

Iron fluxes & budget

Comparing the two resolution runs, we see that the 5 km run resolves eddy fluxes better. The eddy fluxes, particularly vertical, supply iron from depth to the surface (Figs. 8, 9) and the diffusive flux take over near the very surface.

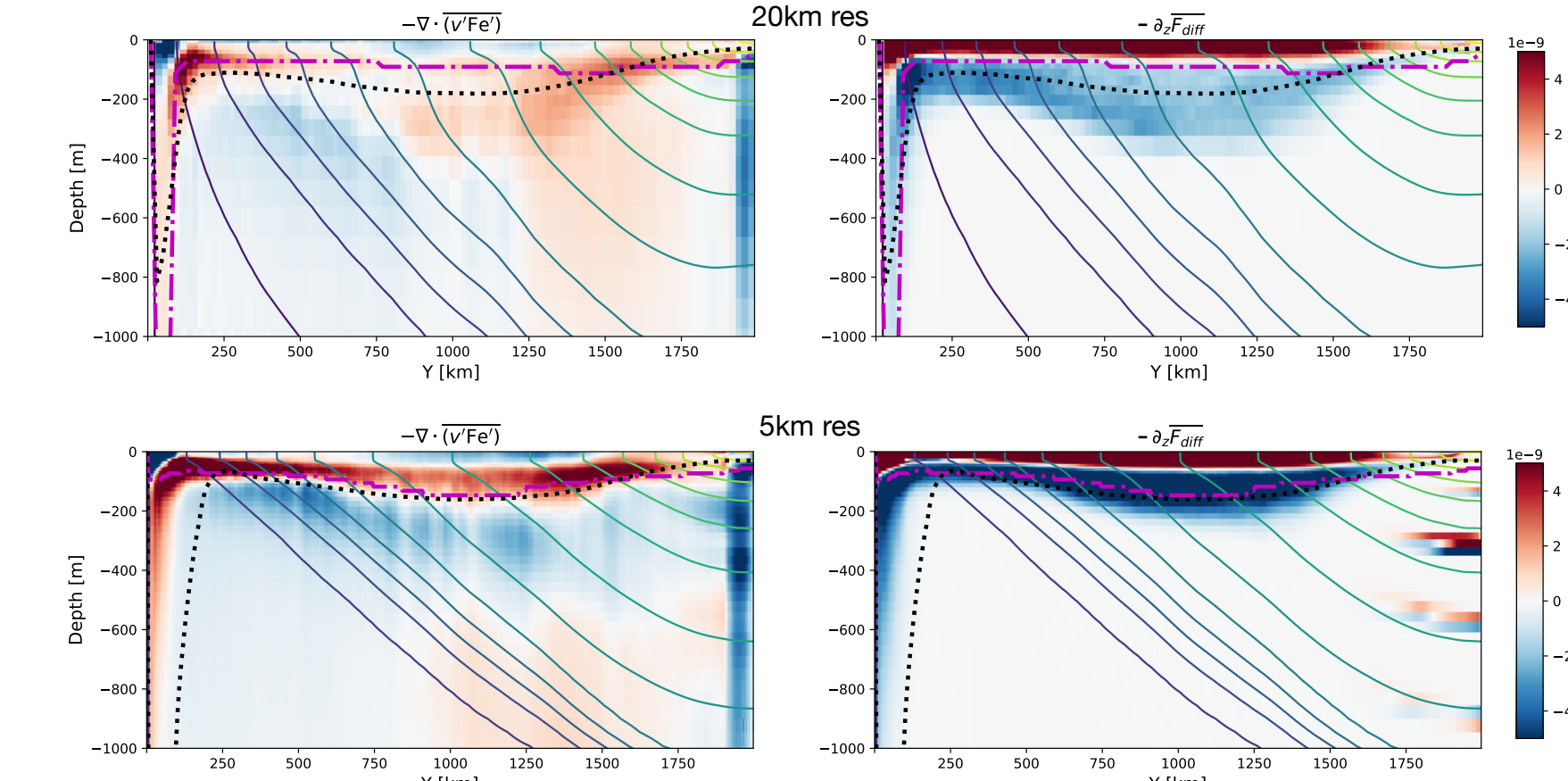


Figure 8: Climatological eddy iron flux convergence and vertical diffusion in the top 1000m.

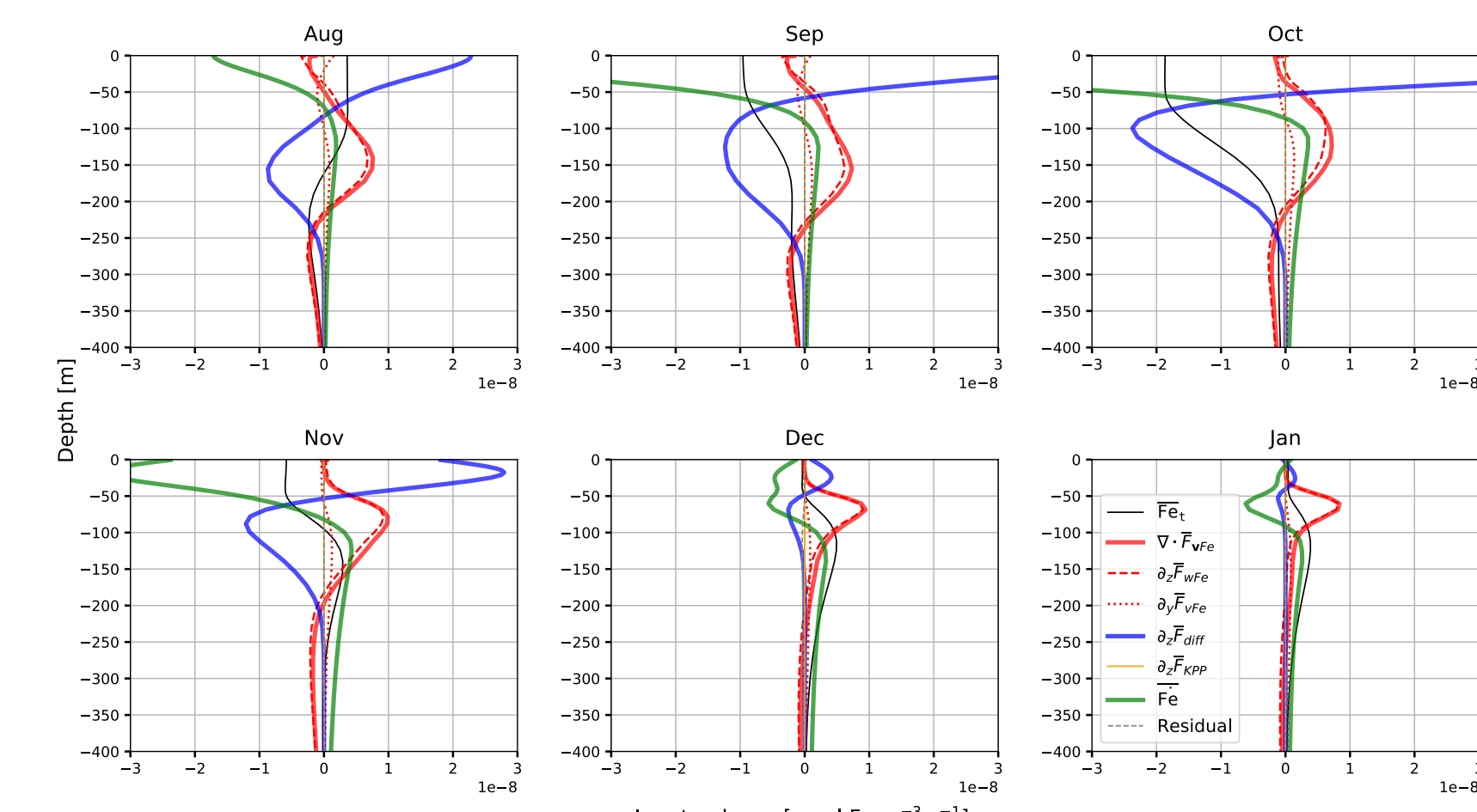


Figure 9: Monthly climatology of the iron budget.

Primary production

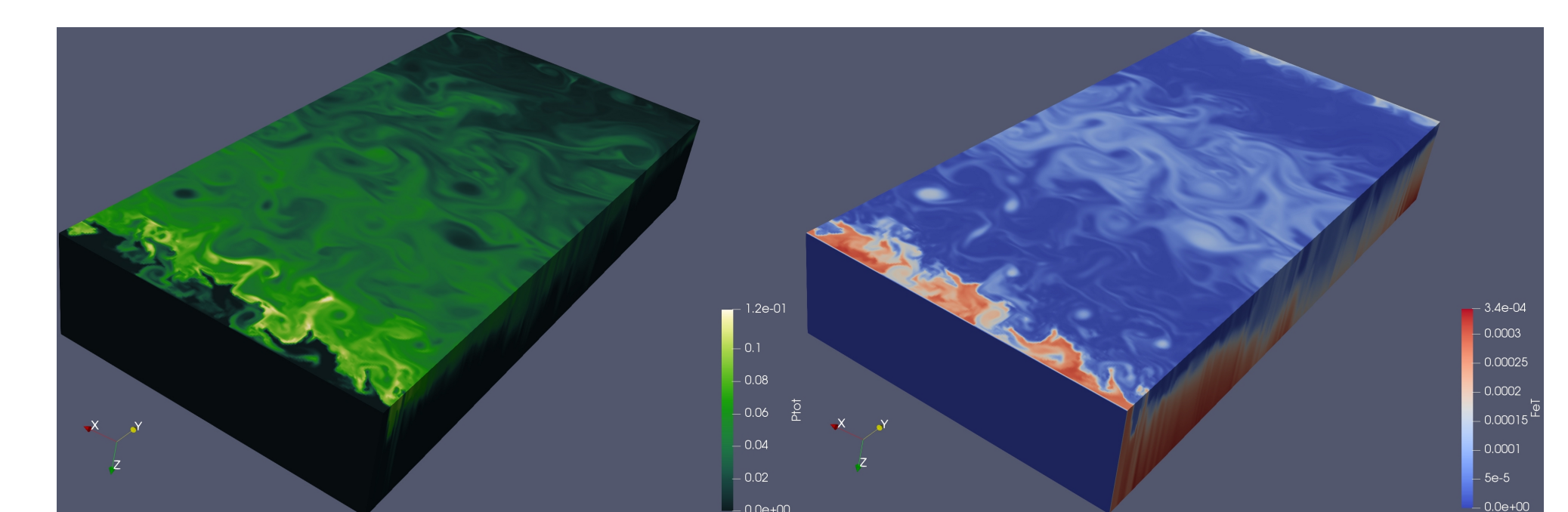


Figure 10: Daily averaged snapshot of total biomass and iron on Oct. 15.

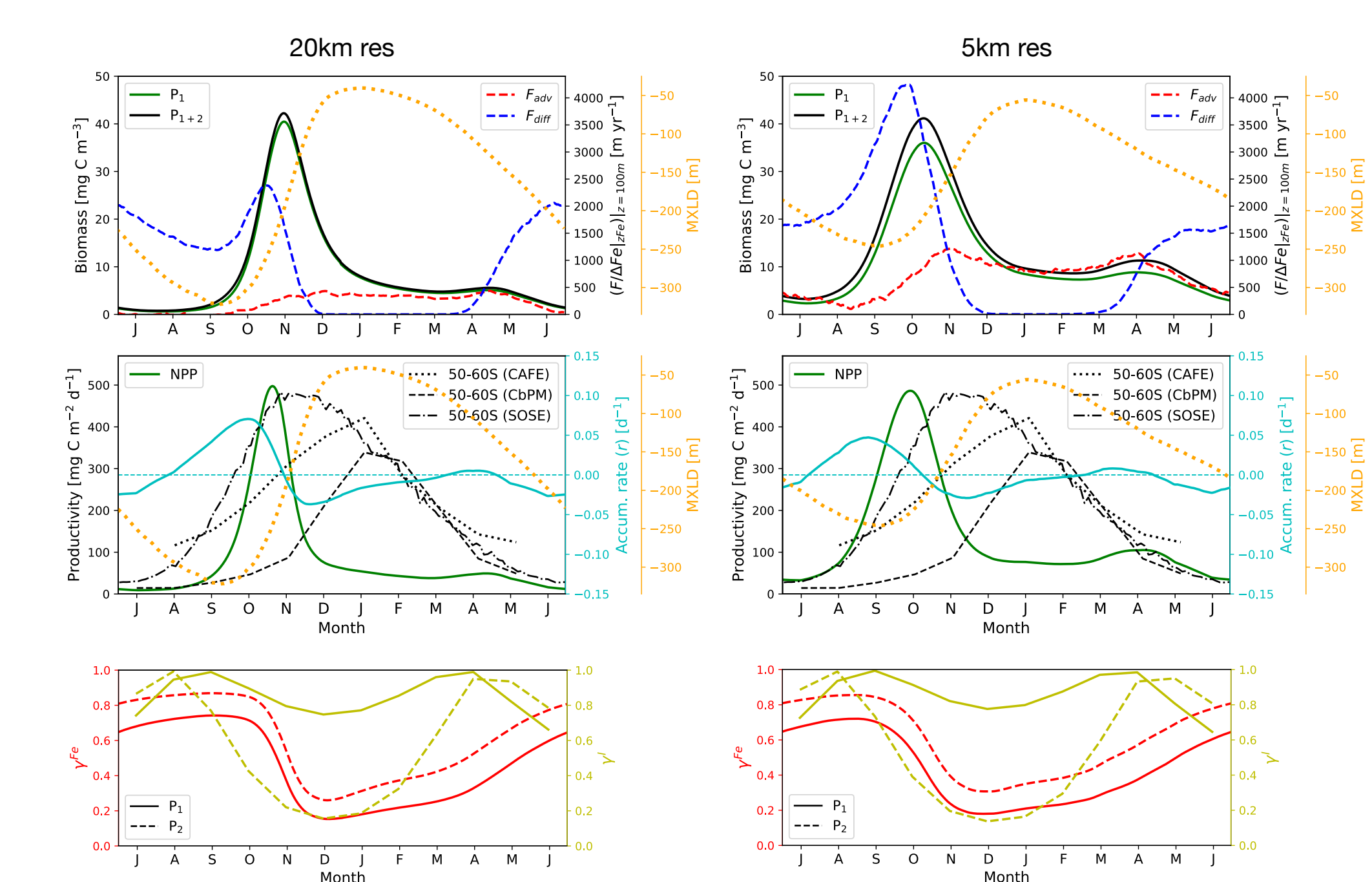


Figure 11: Monthly climatology of biomass, productivity and limiting factors.

The biological parameter were kept the same for both resolution runs to highlight the influence of resolving the mesoscale.

The 20 km run is diffusive and in a sense is close to one-dimensional simulations done by previous studies in the context of Southern Ocean iron supply. We see that the spring bloom is very peaky in the 20 km run as the phytoplankton deplete the iron supplied by winter-time MXL entrainment. The vertical eddy flux in the 5 km run augment the iron supply from depth and allow for a less peaky bloom and also raises the annual baseline of biomass.

The apex of the spring bloom occurs after the MXLD starts to shallow, consistent with previous studies, and iron limitation increases drastically after the bloom initiates. It is interesting to note that the spring bloom in both of our resolutions end too early compared to observational products available but is on the same order of magnitude over autumn and winter. We attribute this to our simulations lacking iron sources other than iron supplied from depth via advective and diffusive fluxes.

Conclusion

Evidence from diagnostics of baroclinic APE conversion rates and linear quasi-geostrophic stability analysis indicate that seasonally varying mixing-layer instability is responsible for the EKE seasonality at scales below 100 km, consistent with satellite observations. Austral winter (JAS) and summer (JFM) are in the same phase of wind stress seasonality so EKE and ML APE conversion is in phase with the surface diabatic forcing.

Coupling our seasonally resolving simulations to the two-species version of Darwin indicates that eddy vertical fluxes are important in bringing iron below the ferricline and sustaining primary production over the year.

Contact Information

- Website: <https://roxyboy.github.io>
- Email: takaya@ldeo.columbia.edu